Stochastic Lattice Model Simulations of Molecularly Imprinted Polymers

Xiangyang Wu, William R. Carroll, and Ken D. Shimizu*

Department of Chemistry and Biochemistry, University of South Carolina, Columbia, South Carolina 29208

Received January 26, 2008. Revised Manuscript Received April 24, 2008

A stochastic computer model was developed that simulates the formation and binding properties of molecularly imprinted polymers (MIPs). This simulation allowed examination of possible mechanisms in the imprinting process. The simulation enabled the rapid study of each variable in the imprinting process, which is difficult to do experimentally because of the interdependence of the variables. In particular, the simulation allowed examination of influence of binding site heterogeneity on the imprinting effect and on the binding properties of MIPs. The simulation was based on a lattice model in which monomer, template, cross-linker, and solvent units occupy positions in a square grid. A stochastic algorithm was utilized to position the monomer and template units in the lattice matrix based on the monomer−template binding constant. The lattice model simulation provides a method to study the imprinting mechanism and also to rapidly optimize the imprinting process. The model was able to simulate the imprinting effect as evidenced by a higher population of high-affinity binding sites in polymers made with the presence of template units. The lattice model simulation was also able to accurately reproduce the structural and energetic binding site heterogeneity of MIPs. Next, the effects of changing the imprinting variables such as the monomer−template stoichiometry and association constant were examined. Again, the simulated MIPs displayed the same trends as experimental MIPs formed under similar imprinting conditions. Finally, the simulation was carried out with isomeric template units to examine the origins of selectivity in MIPs. A clear preference for the imprinted isomer was observed. The ability of this lattice model to accurately replicate the binding properties of MIPs gives credence to the importance of binding site heterogeneity in determining the binding properties of MIPs. The simulation gives support for the hypothesis that the diverse mixture of monomer−template complexes in the prepolymerization mixture is a major source of binding site heterogeneity in MIPs. The simulation suggests new mechanisms and strategies for improving the imprinting effect such as the careful optimization of the statistical ratios of monomer and template or the introduction of blocking groups to reduce the number of low-affinity background binding sites.

Introduction

Introduction to Molecular Imprinted Polymers (MIPs). The molecular imprinting technique is a template based approach for preparing polymers with tailored recognition properties.[1–5] In the molecular imprinting process, a polymerization is carried out in the presence of a template molecule (Scheme 1). Removal of the template from the highly cross-linked polymer matrix creates binding sites with shape and functional group complementarity to the template molecule. This approach has received extensive attention in recent years due to its advantages of synthetic efficiency, chemical and thermal stability, and low cost.[6] The imprinting process has been successfully applied to a wide range of templates including: pharmaceuticals, pesticides, herbicides, carbohydrates, transition state analogues, and even proteins.[1,2,7] The synthetic efficiency and adaptability of the imprinting process has facilitated the use of MIPs in many applications including: enantiomeric separation,[8,9] solid-phase extraction,[10,11] and sensing.[12,13] A major difficulty, however, in the development of molecularly imprinted materials is a lack of a clear understanding of the imprinting process. This has hampered the optimization and rational improvement of new imprinted materials. To assist in studying and improving the imprinting process, we have developed a simple lattice model simulation of the molecular imprinting process. The simula-

* Corresponding author. Tel.: +01 803 777 6523. Fax: +01 803 777 9521. E-mail: shimizu@mail.chem.sc.edu.

(1) Alexander, C.; Andersson, H. S.; Andersson, L. I.; Ansell, R. J.; Kirsch, N.; Nicholls, I. A.; O'Mahony, J.; Whitcombe, M. J. *J. Mol. Recognit.* **2006**, *19*, 106–180.
(2) Wulff, G. *Chem. Rev.* **2002**, *102*, 1–27.
(3) Yan, M.; Ramstrom, O. *Molecularly Imprinted Materials: Science and Technology*; Marcel Dekker: New York, 2005; p 734.
(4) Sellergren, B. *Molecularly imprinted polymers: man-made mimics of antibodies and their applications in analytical chemistry*; Elsevier: Amsterdam; New York, 2001; p 557.
(5) Shea, K. J. *Trends Polym. Sci.* **1994**, *2*, 166–173.
(6) Wulff, G. *Angew. Chem., Int. Ed. Engl.* **1995**, *34*, 1812–1832.
(7) Zimmerman, S. C.; Lemcoff, N. G. *Chem. Commun.* **2004**, 5–14.
(8) Spivak, D. A. *Adv. Drug Delivery Rev.* **2005**, *57*, 1779–1794.
(9) Maier, N. M.; Lindner, W. *Anal. Bioanal. Chem.* **2007**, *389*, 377–397.
(10) Lanza, F.; Sellergren, B. *Chromatographia* **2001**, *53*, 599–611.
(11) Qiao, F. X.; Sun, H. W.; Yan, H. Y.; Row, K. H. *Chromatographia* **2006**, *64*, 625–634.
(12) Takeuchi, T.; Haginaka, J. *J. Chromatogr., B* **1999**, *728*, 1–20.
(13) Haupt, K.; Mosbach, K. *Chem. Rev.* **2000**, *100*, 2495–2504.

10.1021/cm8002645 CCC: $40.75
Published on Web 06/14/2008

Scheme 1. Schematic Representation of the Molecular Imprinting Process, Highlighting BSH in the Imprinted Polymer, and Its Origins in the Mixture of Monomer−Template Complexes in the Prepolymerization Solution[a]

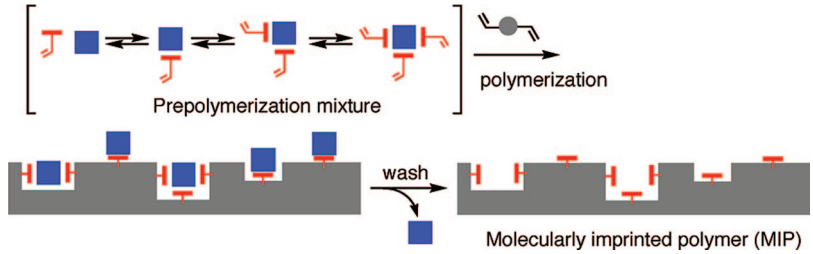

[a] The template, functional monomer, and crosslinker are depicted in blue, red, and grey, respectively.

tion is based on the thermodynamic equilibrium processes in the imprinting process. A key aspect of the simulation was the ability to study and measure the influence of binding site heterogeneity (BSH) on the binding properties of MIPs. The model was also able to reproduce experimentally observed trends in binding properties and thus can be used to rapidly examine different variables and to optimize the imprinting process.

Despite its apparent simplicity, the imprinting process is a mechanistically complex process (Scheme 1). The template, the functional monomer, and the cross-linker are typically mixed together in a solvent. In this prepolymerization solution, the template is in dynamic equilibrium with the functional monomer, forming many types of monomer−template complexes of varying stoichiometry and structure. The polymerization process captures the different monomer−template complexes within a rigid polymer matrix. In the last step, the template is washed out of the cross-linked polymer matrix. The overall imprinting process is a balance between the thermodynamic processes in the prepolymerization solution and the kinetic processes that occur during polymerization. The many variables in the imprinting process, such as temperature, concentration, solvent, and stoichiometry, are all highly interdependent. This interdependence of the imprinting variables has made the rational optimization and study of the imprinting process a difficult problem to address experimentally.[14,15] Changing any one variable will affect both the thermodynamic equilibrium and the polymerization kinetics. For example, increasing or decreasing the solvent polarity will simultaneously shift the monomer−template equilibrium and also alter the morphology of the polymer matrix, and both of these factors will collectively alter the binding properties of the imprinted polymer.

In this study, we have developed a stochastic computer model to simulate and study the imprinting process in a more controlled environment. The model is a lattice model simulation in which the components of an MIP (monomer, template, and cross-linker) occupy positions in a two-dimensional square grid. The model focuses on simulating the thermodynamic equilibrium processes in the prepolymerization solution and examines their influences on the binding properties of MIPs. Despite the course-grained nature of the model, it was able to accurately reproduce the imprinting effect and the experimentally observed trends in their binding properties as will be demonstrated vide infra. The model serves two purposes. First, it allows rapid optimization of the imprinting process. Second, it can be used to study the imprinting mechanism. In particular, we were specifically interested in the importance of BSH on the binding properties of MIPs.[16,17] A central aspect of the model is simulating the BSH in MIPs. We believe that the inclusion of BSH into this model is a key reason why it is able to reproduce the imprinting effect and binding property trends.

The most common method for preparing MIPs utilizes monomers and templates that form noncovalent interactions such as hydrogen-bonding, electrostatic, $\pi-\pi$ stacking, hydrophobic, and van der Waals interactions.[18,19] The noncovalent imprinting method is synthetically efficient as the monomer−template complexes are formed in situ in the prepolymerization mixture, as shown in Scheme 1. The noncovalent interactions are also relatively weak and are reversible, which leads to the formation of many different monomer−template complexes with varying monomer−template stoichiometries and structures. The focus of our simulation will be on modeling the equilibrium processes in the prepolymerization solution because we believe that they are the primary sources of the imprinting effect and also of the BSH. For example, variables that influence the monomer−template binding equilibrium such as monomer concentration, template concentration, and monomer−template association constants have been shown to have a profound impact on the binding properties of MIPs.[14,15]

Further complicating the study of molecularly imprinted materials is their heterogeneous structure, and this unique characteristic is incorporated into the simulation. Imprinted polymers contain many different types of binding sites. As a result, MIPs cannot be characterized by a single set of binding parameters such as the number of binding sites (N) or binding affinity (K). Instead, each binding site in an MIP has its own set of binding parameters (K_i, N_i). This

(14) Davies, M. P.; De Biasi, V.; Perrett, D. *Anal. Chim. Acta* **2004**, *504*, 7–14.
(15) Rosengren, A. M.; Karlsson, J. G.; Andersson, P. O.; Nicholls, I. A. *Anal. Chem.* **2005**, *77*, 5700–5705.
(16) Rampey, A. M.; Umpleby, R. J.; Rushton, G. T.; Iseman, J. C.; Shah, R. N.; Shimizu, K. D. *Anal. Chem.* **2004**, *76*, 1123–1133.
(17) Shimizu, K. D. *Mater. Res. Soc. Symp. Proc.* **2002**, *723*, 17–21.
(18) Mosbach, K.; Haupt, K. *J. Mol. Recognit.* **1998**, *11*, 62–68.
(19) Ramstrom, O.; Nicholls, I. A.; Mosbach, K. *Tetrahedron: Asymmetry* **1994**, *5*, 649–656.

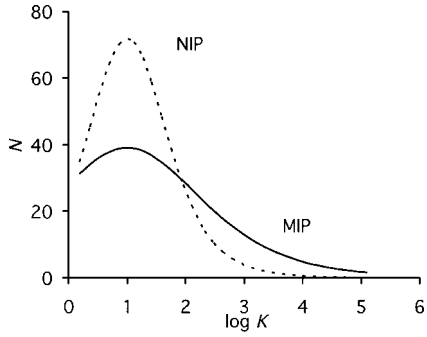

Figure 1. Affinity distributions of an MIP formed in the presence of a template molecule and a nonimprinted polymer (NIP) formed in the absence of a template.

heterogeneous population of binding sites is commonly characterized using an affinity distribution (N, log K).[20] Figure 1 shows the typical broad asymmetric distribution of the binding energies within an MIP, which typically spans many orders of magnitude. The majority of binding sites have low affinity for the template molecule. However, the distribution also tails into the high affinity region where MIPs have a small but important population of high-affinity, high-selectivity binding sites. These high-affinity binding sites are formed by the template in the imprinting process. Our interests in BSH in MIPs stem from our experimental studies on MIPs.[20–22] We have observed that BSH not only attenuates the binding properties of MIPs but also may contribute to the imprinting effect. For example, imprinted polymers typically have greater BSH than their corresponding nonimprinted polymers (NIPs) as shown in Figure 1. The broader more heterogeneous distributions of MIPs ensure that there will be a significant population of the rare high-affinity binding sites in MIPs especially in comparison to NIPs.

BSH influences every aspect of an MIP's binding properties. BSH also complicates the experimental measurement and comparison of the binding properties of MIPs. This is because BSH makes the measured binding properties of MIPs highly dependent upon the conditions and concentrations in which they were measured. This variability makes the comparison of MIP binding properties a very complex analysis. For example, an MIP usually displays very high selectivities at low analyte concentrations and low selectivities at high analyte concentrations. Other binding properties such as association constant and binding capacity are also highly concentration dependent. The reason for this wide variation in observed binding properties is because different subsets of binding sites are being measured at different analyte concentrations. Collectively, these factors make it very difficult to accurately measure and compare the binding properties of MIPs.

Due to these experimental challenges in characterizing MIPs, the imprinting process has also been studied using computational modeling and simulations. Two general types of computer modeling have been applied to the molecular imprinting problem. The first are molecular modeling simulations that calculate the structure and stability of monomer−template complexes in the prepolymerization solutions.[23–27] These simulations yield an estimation of the strength and stoichiometries of individual monomer−template complexes. However, these molecular modeling studies do not generally take into account the structural heterogeneity in MIPs. An exception is a recent simulation of the imprinting process carried out by Peppas et al. in which the thermodynamic and kinetic aspects of imprinted polymer formation were iteratively modeled using molecular modeling software.[28,29] The second type of computational models that have been used to study imprinting are course-grained mathematical models. These can simulate polymeric properties such as cross-linker rigidity, cross-linking density, size of template, and porogen. For example, Screbnik et al. have used mean-field polymer lattice models to describe and study the variables in the molecular imprinting process.[30–32] Ito et al. have also modeled imprinted materials using a fixed point model of the polymer matrix.[33]

While these lattice models do not have the atomic-level accuracy of molecular modeling studies, they do have the ability to model the breadth of the structural variations in MIPs. Thus, we were interested in developing a simple lattice model to examine the origins and influence of BSH in MIPs. The initial goals were to (1) study the origins of BSH in MIPs and (2) to study the link between BSH and the imprinting effect. In the course of these studies, we found that our lattice model simulations were able to replicate the experimentally observed binding properties of MIPs with a surprising degree of accuracy. The variables for the formation of the simulated imprinted polymers are analogous to those of experimental imprinted polymers. Thus, experimental imprinting studies in the literature could be simulated using our stochastic model for comparison. The simulation could also be used to examine the variables in the imprinting process such as monomer/template stoichiometric ratios, concentrations, and binding affinities.

Theory

Basis for the Model. The MIP simulation was constructed on a two-dimensional lattice, which represents the surface of an imprinted polymer. Lattice models are widely used in

(20) Umpleby, R. J., II; Bode, M.; Shimizu, K. D. *Analyst* **2000**, *125*, 1261–1265.
(21) Rushton, G. T.; Karns, C. L.; Shimizu, K. D. *Anal. Chim. Acta* **2005**, *528*, 107–113.
(22) Umpleby, R. J., II; Baxter, S. C.; Chen, Y.; Shah, R. N.; Shimizu, K. D. *Anal. Chem.* **2001**, *73*, 4584–4591.
(23) Wu, L. Q.; Sun, B. W.; Li, Y. Z.; Chang, W. B. *Analyst* **2003**, *128*, 944–949.
(24) Piletsky, S. A.; Karim, K.; Piletska, E. V.; Day, C. J.; Freebairn, K. W.; Legge, C.; Turner, A. P. F. *Analyst* **2001**, *126*, 1826–1830.
(25) Takeuchi, T.; Dobashi, A.; Kimura, K. *Anal. Chem.* **2000**, *72*, 2418–2422.
(26) Dong, W. G.; Yan, M.; Liu, Z.; Wu, G. S.; Li, Y. M. *Sep. Purif. Technol.* **2007**, *53*, 183–188.
(27) Wei, S.; Jakusch, M.; Mizaikoff, B. *Anal. Bioanal. Chem.* **2007**, *389*, 423–431.
(28) Henthorn, D. B.; Peppas, N. A. *Ind. Eng. Chem. Res.* **2007**, *46*, 6084–6091.
(29) Oral, E.; Peppas, N. A. *Polymer* **2004**, *45*, 6163–6173.
(30) Srebnik, S.; Lev, O. *J. Chem. Phys.* **2002**, *116*, 10967–10972.
(31) Yungerman, I.; Srebnik, S. *Chem. Mater.* **2006**, *18*, 657–663.
(32) Srebnik, S. *Chem. Mater.* **2004**, *16*, 883–888.
(33) Ito, K.; Chuang, J.; Alvarez-Lorenzo, C.; Watanabe, T.; Ando, N.; Grosberg, A. Y. *Prog. Polym. Sci.* **2003**, *28*, 1489–1515.

Scheme 2. Portion of the Square Lattice of the Imprinted Polymer Simulation Containing Solvent, Template, Monomer, and Crosslinker Units

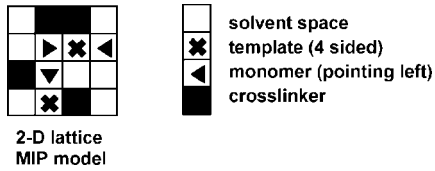

simulating adsorption and polymer properties.[34,35] For example, lattice models form the basis for the Langmuir adsorption isotherm and Flory's polymer models for polymer properties.[36] Two-dimensional lattice models are commonly used to simulate adsorption phenomenon because concentration scales linearly from three dimensions to two dimensions.

In the MIP simulation, the lattice is populated with four types of units as shown in Scheme 2. These are the monomer, template, cross-linker, and solvent units. Each unit is the same size and occupies one square in the lattice. The monomer unit is directional and can form interactions with only one of the four adjacent spaces. The binding face of the monomer unit is denoted graphically by the point of the triangle. The template molecule (shown as a cross) have four binding faces and can therefore bind up to four adjacent monomers. The cross-linker, in contrast, has no affinity for the monomer or template unit in this model. The simulation is a static model. The individual units have no mobility or flexibility once they are positioned in the matrix.

A key assumption in this simulation was that the monomer−template complexes in the prepolymerization mixture are quantitatively captured by the polymerization process and frozen in the rigid polymer matrix. This assumption was based on the observation that variables that affect the monomer−template equilibrium have a profound influence on the imprinting effect. Variables in the polymerization process such as the cross-linker density and polymer solvation are also known to have an influence on the imprinting factor. However, these polymeric factors do not give rise to the imprinting effect and only modulate the imprinting effect.

The monomer−template equilibrium was simulated using a stochastic algorithm that positions the monomer and template units in the lattice, depending upon their binding affinities.[37–39] The basis for the algorithm is eq 1, which expresses the microscopic monomer−template association constant (K^*) in terms of the probability term ρ_1. This equation is derived from the microscopic partition equilibrium (eq 2) in which each monomer unit (M) is either free or bound to a template unit. The variables, ρ_1 and ρ_{-1}, are the probabilities that a free monomer becomes a bound monomer or that a bound monomer becomes a free monomer. Thus, the microscopic binding constant, K^*, for the monomer−template equilibrium can be defined as the ratio of ρ_1 and ρ_{-1} (eq 3). Each monomer unit must be either free or bound, and therefore, the sum of ρ_1 and ρ_{-1} must be 1 (eq 4). Combining eqs 3 and 4 yields eq 1.

Scheme 3. Four Steps of the Simulated Imprinting Process Followed by the Analysis of the Binding Sites in the *s*MIP[a]

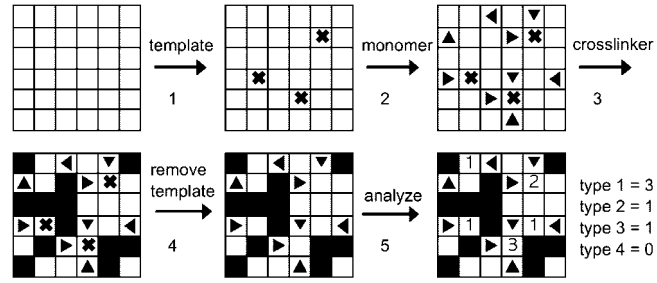

[a] The binding sites were tabulated and organized into types 1, 2, 3, and 4 representing the number of monomers lining the binding site. In step five, the binding sites in the *s*MIPs are analyzed.

$$K^* = \frac{\rho_1}{1-\rho_1} \tag{1}$$

$$M_{\text{free}} \underset{\rho_{-1}}{\overset{\rho_1}{\rightleftharpoons}} M_{\text{bound}} \tag{2}$$

$$K^* = \frac{\rho_1}{\rho_{-1}} \tag{3}$$

$$\rho_1 + \rho_{-1} = 1 \tag{4}$$

The probability-based algorithm was used to position the individual monomer units in the simulation. The stochastic nature of the algorithm allows it to be easily scaled to different lattice sizes and monomer−template stoichiometries. The accuracy of eqs 1 and 2 were verified by their ability to accurately replicate complex binding equilibrium. The concentrations of various monomer−template complexes were stochastically calculated using the above equations. These values were compared to the concentrations for the same input variables calculated using the macroscopic binding equilibrium equations and an excellent correlation was observed (see Supporting Information).

Implementation of the Model. A computer program was written in Matlab based on eq 1. A flowchart of the program is provided in the Supporting Information. The imprinting process was broken up into four separate steps (Scheme 3). In the first three steps, the template, monomer, and crosslinker units were successively placed in the lattice. In step four, the template units were removed from the lattice. Finally the simulated MIP (*s*MIP) was analyzed. The empty spaces in the lattice were evaluated with respect to their ability to rebind the template, and the populations of these different binding sites were tabulated. Binding sites were defined, as open squares that are bordered by one or more sides by monomer units that are appropriately oriented to form a binding interaction with the open space. The quality of a binding site depended on the number of adjacent monomers that can form binding interactions with a template

(34) Holm, C.; Kremer, K. *Advanced computer simulation approaches for soft matter sciences 1*; Springer: Berlin, 2005; pp x, 275.
(35) Binder, K. *Monte Carlo and molecular dynamics simulations in polymer science*; Oxford University Press: New York, 1995; pp xiv, 587.
(36) Vanderzande, C. *Lattice models of polymers*; Cambridge University Press: Cambridge, 1998; pp xii, 222.
(37) Mcquarrie, D. A. *J. Appl. Prob.* **1967**, *4*, 413–478.
(38) Veitl, M.; Schweiger, U.; Berger, M. l. *Comput. Biomed. Res.* **1997**, *30*, 427–450.
(39) Hubble, J. *Biotechnol. Prog.* **2001**, *17*, 565–567.

in the binding site. These are denoted in the analyzed *s*MIP with numbers 1−4. Thus, there are four types of binding sites in the simulation: types 1, 2, 3, and 4 that are lined with one, two, three, and four adjacent functional monomers (Scheme 3).

The number and positioning of each unit is dependent upon the input variables for the simulation. The input variables for the *s*MIP are analogous to those of experimental MIPs. These are the concentrations of template ([T]), monomer ([M]), and cross-linker units ([CL]) and the microscopic monomer−template association constant (K^*). The template and cross-linker units (steps 1 and 3) were randomly placed into empty positions in the lattice. The key step in the simulation was the placement of the monomer units (step 2), which is dependent on the microscopic binding constant. The probability of placing a monomer unit in an empty space was dependent on whether the monomer could form a binding interaction with an adjacent template molecule. The probability of placing monomer in a space where it can form a binding interaction is ρ_1 and the probability of placing a monomer in a space where it cannot form a binding interaction is ρ_{-1}. The values of ρ_1 and ρ_{-1} were assigned from the input parameter K^* using eq 3.

The concentration units for the simulation are in number of units per total number of squares in the simulation lattice. Since the concentrations are expressed in number of units versus number of units which cancel each other out, the concentrations and also the binding constant (K^*) have no formal units. These concentrations are expressed as percentages, which correlate to the fraction of the total lattice area occupied by each unit. These concentration units can be correlated to experimental concentration units of volume fraction or mole fraction.

Results and Discussion

The imprinting simulation was tested under a variety of conditions. The purpose of these studies was threefold. The first was to study the origins of the imprinting effect and, in particular, to examine the influence of BSH on the imprinting effect. The second goal was to utilize the simulation to examine the influence of each variable in the imprinting process on the imprinting effect. The third goal was to study the influence of different variables on the selectivity of MIPs.

To accomplish these goals, four sets of experiments were carried out that compared the binding properties of the MIPs reported in the literature. These comparative studies were facilitated by the ability to directly compare the input and output variables from the simulation with those reported in the literature for experimental MIP systems. The first study examined whether an imprinting effect was present in the *s*MIPs. The second study tested whether the *s*MIPs had a similar binding site distribution to experimental MIPs. The third study evaluated whether the simulated imprinting process was able to accurately reproduce changes in the imprinting conditions. The fourth study tested whether the lattice model simulation could model the selectivity of MIPs.

1. Comparison of Simulated Imprinted and Nonimprinted Polymers. Study one compared the differences between a simulated imprinted and nonimprinted polymer (*s*MIP1 versus *s*NIP). These are systems made with identical input parameters of monomer concentration (M), template concentration (T), and cross-linker concentration (CL). The only input variable that was varied was the microscopic association constant (K^*). The variables of template, monomer, and cross-linker concentrations were held constant ([T] = 1.95%, [M] = 7.81%, [CL] = 31.25%). These concentrations and stoichiometry correspond to typical molecular imprinting conditions reported in the literature, which have a 1:4:16 = template:monomer/cross-linker ratio and a total volume of monomer plus cross-linker that make up approximately 1/3 of the entire prepolymerization solution.[40] For *s*NIP, K^* was set to 1, which simulates a polymer in which the monomer has no binding affinity for the template. Thus, the template in *s*NIP is effectively another solvent molecule. For *s*MIP1, K^* was set to 33.3. This value of K^* for *s*MIP1 falls within the range of a typical monomer−template binding constant (10^1 to 10^2 M^{-1}).[41]

One advantage of the lattice model simulation is that the imprinting process and completed *s*MIP and *s*NIP can be visually evaluated. Scheme 4 shows representative (16 × 16) subsets of *s*NIP and *s*MIP1 lattices. The graphical output yields a microscopic view of the imprinted and nonimprinted polymers. The empty spaces that form binding sites are classified by the number of functional monomers lining the binding site and are labeled with numbers 1−4. Both the number and distribution of binding sites in *s*MIP1 and *s*NIP are consistent with experimental studies of the imprinting effect. *s*MIP1 and *s*NIP have similar overall number of binding sites (12 vs 11). However, *s*MIP1 has a higher population of high-affinity binding sites (types 2, 3, 4) that contain two or more functional monomer units. These subtle differences in the populations of the high-affinity binding sites are consistent with experimentally observed distribution of binding sites in MIPs.

An advantage of being able to visualize the imprinting process is that origins of each binding site can be monitored. Binding sites can be formed either by a template unit or randomly by the placement of one or more monomer units next to an empty space with the right orientation. These differences are seen in Scheme 4. Binding sites that were previously occupied by template units are highlighted in gray. As expected, the majority of binding sites in *s*NIP are not gray and were formed randomly by the monomer units. In *s*NIP, presence of a template unit does not increase the probability of forming binding sites because there is no affinity for the monomer units in *s*NIP. In contrast, approximately half of the binding sites in *s*MIP1 were formed around a template unit. This means that approximately half of the binding sites were also formed randomly. The preponderance of these randomly formed binding sites is consistent with the high population of background or low-affinity binding sites observed in imprinted materials. The origins of the binding sites in *s*MIP1 are also not weighted equally among the different types of binding sites. Like *s*NIP, the majority of low-affinity (type 1) binding sites in *s*MIP1 were formed randomly. However, the opposite was true for

(40) Spivak, D.; Shea, K. J. *J. Org. Chem.* **1999**, *64*, 4627–4634.
(41) Wulff, G.; Knorr, K. *Bioseparation* **2001**, *10*, 257–276.

Scheme 4. Screenshots of (left) *s*NIP ($K^* = 1$) and (right) *s*MIP1 ($K^* = 33.3$)[a]

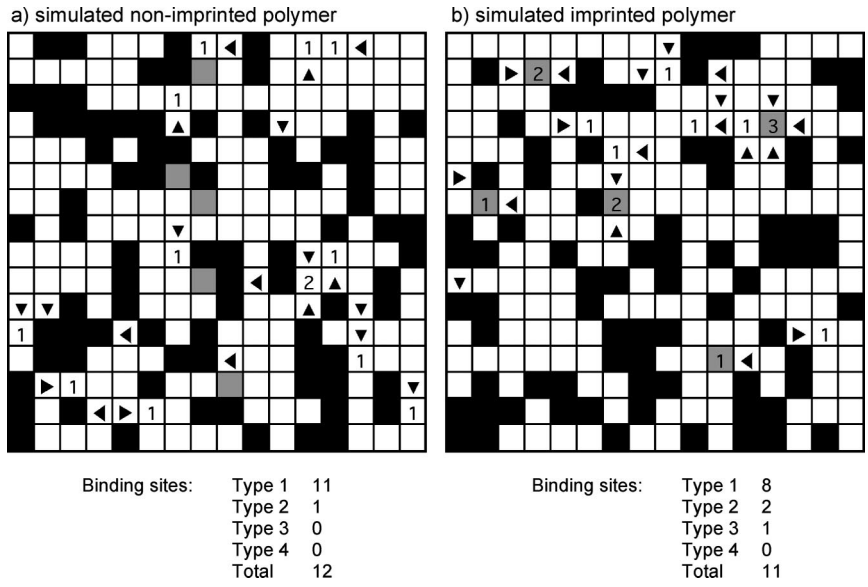

[a] Empty squares that form binding sites are denoted with a number corresponding to the number of functional monomers lining the binding site. Empty squares that were previously occupied by a template unit are highlighted in grey.

the high-affinity binding sites (types 2, 3, 4). The majority of these high-affinity binding sites were formed by the template unit. These simulations demonstrate that the imprinting process proceeds with relatively low fidelity because half of the binding sites in *s*MIP1 are low-affinity sites formed randomly and not via the imprinting process.

Next, the influence of the cross-linker on the simulated imprinting process was examined. The role of the cross-linker in this simulation is relatively limited. The cross-linker does not directly contribute to the binding energy of a binding site. The cross-linker also does not attenuate the rigidity of the polymer matrix. However, the cross-linker still influences the simulated imprinting process by acting as a blocking unit. The cross-linker can occupy and block the binding faces of the monomer or template units. In *s*NIP, approximately 35% of the monomers are blocked by cross-linkers or by other monomer units. In *s*MIP1, this number is significantly lower (25%) due to the competition of the template unit for the binding faces of the monomer units. Thus, the cross-linker in this simulation is beneficial because it actually reduces the number of low-affinity binding sites that are randomly formed by occupying the monomers that are not bound to a template unit. This role as a blocking unit suggests a new route to improve the imprinting effect. A cross-linker or another monomer could be added to occupy the monomer units that are not bound to a template leading to a reduction in the number of low-affinity binding sites. This mechanism may also help to explain the popularity and effectiveness of carboxylic acid and primary amide monomers such as methacrylic acid and methacrylamide in the imprinting process. Both of these monomers self-associate in solution to form dimers. The MIP simulation suggests that this self-association effectively reduces the number of low-affinity binding sites in the MIPs prepared from these monomers.

A more careful statistical analysis of *s*MIP1 ($K^* = 33.3$), *s*MIP2 ($K^* = 50$), and *s*NIP ($K^* = 1$) was carried out by extending the simulation to a larger lattice containing 1×10^8 squares. These larger lattice dimensions ensured that the simulation would yield stable results as type 3 and type 4 binding sites that occur with lower probability would be formed in statistically relevant numbers. The numbers and types of binding sites for each simulated polymers are tabulated in Table 1. The subtle differences in the distribution of binding sites are more clearly discernible in Table 1, which shows the percentages of each type of binding site and the total number of binding sites in the respective polymers. The *s*MIPs have fewer low-affinity (type 1) binding sites than *s*NIP. However, these low-affinity binding sites still make up the majority of binding sites in the *s*MIPs. More dramatic differences are seen in the population of high-affinity binding sites containing two or more monomer units. These high-affinity binding sites represent only 2.8% of the total number of binding sites in *s*NIP in comparison to 14% of the binding sites in *s*MIP1 and 17% in *s*MIP2. As expected, *s*MIP2 with the higher K^* has more high-affinity binding sites than *s*MIP1 with the lower K^*. These differences in population become larger with increasing affinity of the binding site. For example, *s*MIP2 has 1.6 times as many type 3 binding sites as *s*MIP1 and has 2.2 times as many type 4 binding sites.

The lattice model simulation also allows rapid analysis of the change in the distribution over a wide range of imprinting conditions. For example, the influence of K^* on the imprinting effect and the distribution of binding sites was examined

Table 1. Distribution of Binding Sites in *s*NIP ($K^* = 1$), *s*MIP1 ($K^* = 33.3$), and *s*MIP2 ($K^* = 50$) with Percent of Total Number of Binding Sites in Each Polymer

	type 1 (% of total binding sites)	type 2 (% of total binding sites)	type 3 (% of total binding sites)	type 4 (% of total binding sites)	total number of binding sites (%)
*s*NIP	97.20	2.76	0.04	0	4.635
*s*MIP1	80.45	14.14	4.74	0.67	4.624
*s*MIP2	73.57	16.80	8.06	1.57	4.400

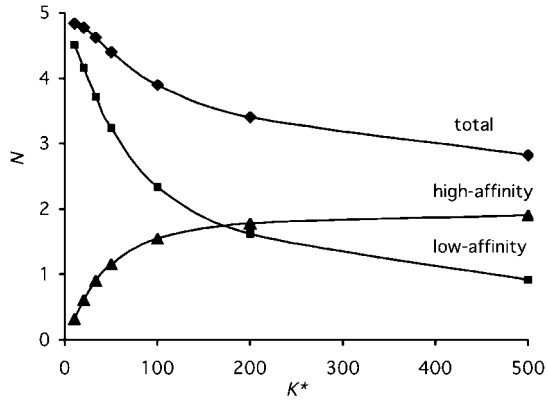

Figure 2. Number of low-affinity (type 1), high-affinity (types 2, 3, 4), and all binding sites (types 1−4) with increasing binding constant (K^*) in the *s*MIPs.

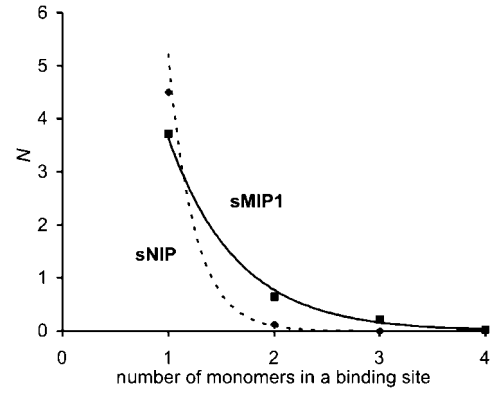

Figure 3. Affinity distributions of *s*NIP ($K^* = 1$) and *s*MIP1 ($K^* = 33.3$).

(Figure 2). The number of high-affinity binding sites (types 2, 3, 4) increases with increasing monomer−template binding constant. This is consistent with the observation that the imprinting effect increases with increasing monomer−template binding constant. Higher monomer−template association constants increase the population of higher order monomer−template complexes, which form the high-affinity binding sites. This is accompanied by a rapid decrease in the number of low-affinity binding sites. We and others have theorized that this might be the case due to the partitioning of the monomer units between the high-affinity and low-affinity binding sites.[42] The formation of each high-affinity binding site in the MIP requires multiple monomer units and thus, fewer monomer units are available to form the low-affinity binding sites. This can also be seen by the decrease in the total number of binding sites with increasing K^*. This higher capacity of the less imprinted materials is very difficult to measure experimentally because the majority of binding sites have very low association constants ($K^* < 10$) that are difficult to accurately measure. This simulation gives us the first confirmation of this phenomenon. It should be noted that Figure 2 suggests that increasing K^* beyond a certain point does not further improve the binding properties as the number of high-affinity sites does not change with $K^* > 100$. However, the relative distribution within these high-affinity sites does change in this plateau region. This will be shown in more detail in the next section. This first set of studies demonstrated that the lattice model imprinting simulation was able to qualitatively reproduce the imprinting effect. The model was also able to simulate the heterogeneity in MIPs. This enables the examination and comparison of heterogeneity in *s*MIPs. The populations of the different types of binding sites could be easily measured and the influence of changing variables in the imprinting process could be assessed.

2. Comparison of the Distribution With Experimentally Observed Distributions. In the second set of studies, we were interested in whether the lattice model simulation could replicate the exponentially decaying shape of the heterogeneous distribution of binding sites in MIPs.[16,20] BSH is commonly characterized using affinity distributions, which are plots of the number of sites versus binding energy (log K). To calculate the affinity distributions of the simulated polymers, we made the assumption that the binding contributions of each monomer were additive to the binding energy of a binding site. Thus, the binding energy of a binding site would be directly proportional to the number of monomers lining the binding site. This assumption is consistent with the studies by Wulff et al. and Shea and Dougherty that have shown that binding sites lined with more monomers had higher binding affinities.[43,44] This has also been shown indirectly via the observation that templates with fewer binding faces have lower affinities and enantioselectivities.

Based on the above assumption, the simulated affinity distributions of *s*MIP1 and *s*NIP were calculated and are shown in Figure 3. The four types of binding sites are equally spaced on the x-axis of the simulated affinity distributions, and the population of each type of binding site is plotted on the y-axis. The affinity distributions of *s*MIP1 and *s*NIP have the same asymptotically decaying distribution, and the same exponentially decaying shape as actual MIPs and NIPs affinity distributions (Figure 1).[16] The exponential shape of the distributions is evident from the linear semilog plots (Figure 4a). In this format, both the simulated and experimental affinity distributions are linear, demonstrating that they share the same exponentially decaying shape.[45] The semilog format also enabled comparison of the BSH and capacities of *s*MIP1 and *s*NIP (Figure 4b). This can be seen by the similarities between the simulated and the experimentally measured semilog affinity distribution plots for MIPs and NIPs. *s*MIP1 has greater BSH and a higher percentage of high-affinity binding sites than *s*NIP. This can be seen by the flatter slope of *s*MIP1 affinity distribution and also by the divergence of *s*MIP1 and *s*NIP distributions at higher binding affinities. The same trends were experimentally observed when comparing the affinity distributions of MIPs and NIPs. The correlation between the simulated and the experimental affinity distributions lends further

(42) Kim, H.; Spivak, D. A. *J. Am. Chem. Soc.* **2003**, *125*, 11269–11275.
(43) Shea, K. J.; Dougherty, T. K. *J. Am. Chem. Soc.* **1986**, *108*, 1091–1093.
(44) Kirchner, R.; Seidel, J.; Wolf, G.; Wulff, G. *J. Inclusion Phenom. Macrocyclic Chem.* **2002**, *43*, 279–283.
(45) Umpleby, R. J., II; Rampey, A. M.; Baxter, S. C.; Rushton, G. T.; Shah, R. N.; Bradshaw, J. C.; Shimizu, K. D. *J. Chromatogr., B* **2004**, *804*, 141–149.

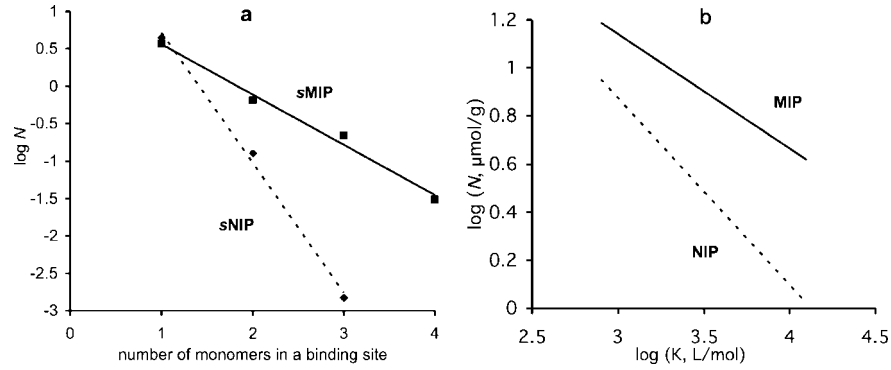

Figure 4. (a) Affinity distributions of *s*NIP ($K^* = 1$) and *s*MIP1 ($K^* = 33.3$) with semilog format; (b) experimental affinity distribution of a real NIP and MIP in log−log format.

credence to the hypothesis that the heterogeneity of the monomer−template equilibrium is a major source of BSH in MIPs.

3. Change in the Magnitude of the Imprinting Effect on Varying Imprinting Conditions. The third set of studies examined whether the lattice model simulation could replicate observed trends in MIPs under varying imprinting conditions. There has been extensive study of the variables in the imprinting process and their influences on the binding properties of MIPs. We focused on two variables, the monomer−template binding constant and the concentration of template. These two variables were chosen for two reasons. First, there are literature studies that examined the influence of these variables on the affinity distribution that could be used for comparison. Second, these variables can be changed without altering the cross-linker percentages. Cross-linker density is known to attenuate the imprinting effect by changing the rigidity of the polymer matrix. However, our simulation does not take into account polymer properties such as rigidity. Therefore, [CL] was kept constant to facilitate accurate comparisons to experimental data.

First, the influence of K^* on the shape of the binding site distribution was examined. We were interested in whether nonexponential distributions could be observed for systems with higher monomer−template association constants. The majority of MIPs in the literature have been prepared using the functional monomers that form weak noncovalent binding interactions ($K < 100\ M^{-1}$).[1,46] MIPs prepared using these low-affinity functional monomers possess a highly heterogeneous distribution of binding sites with an exponentially decaying shape as seen above. More recently, MIPs have been prepared with monomers that form much stronger interactions with the template molecules ($K > 1000\ M^{-1}$).[41,47] MIPs formed from these high-affinity monomers show much lower BSH and have a more unimodal shaped binding site distribution.[20]

These same trends were observed with the *s*MIPs (Figure 5). When the monomer−template binding constant was relatively low ($K^* < 50$), the distribution maintained an exponentially decaying shape. However, when the K^* was greater than 50, a different distribution was observed. At

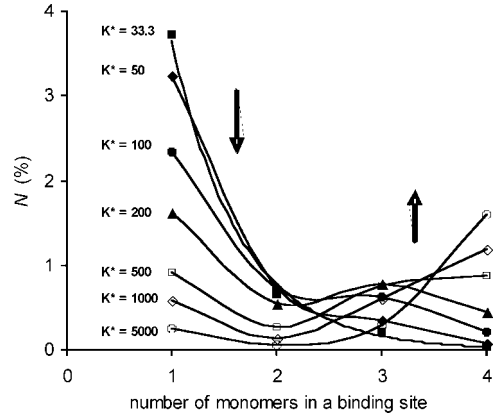

Figure 5. Affinity distributions of *s*MIPs with increasing association constants.

higher association constants, the population of high-affinity binding sites became a significant percentage (75%) of the total number of sites. For example, the highest affinity type 3 and 4 binding sites become the most common type when $K^* = 5000$. Even at lower K^* ($K^* = 100$), a nonexponentially decaying distribution is evident with a clear peak in the distribution. This more homogeneous unimodal distribution observed in the *s*MIPs made with high-affinity monomers is consistent with the observation that MIPs synthesized with monomers that form very strong interactions are also more homogeneous. For example, we have measured the affinity distribution of a covalent MIP.[20] Covalent MIPs are polymers prepared using monomers that are covalently attached to the template molecule. This represents the extreme of a high-affinity monomer. This covalent MIP displayed a unimodal distribution much like the distributions of the *s*MIPs with $K^* > 100$.

The second variable that was examined was template concentration. This variable was particularly attractive because there was an excellent experimental study that could be used for comparison on the influence of template concentration on an MIP's binding properties. Kim and Spivak carried out a study in which the template concentration was varied over a wide concentration range and the population of binding sites with binding affinities between 300 and 10 000 M^{-1} were measured.[42] An unexpected trend was observed. The number of binding sites initially increased with increasing template concentration as expected. However, at higher template concentrations the number of sites rapidly

(46) Tunc, Y.; Hasirci, N.; Yesilada, A.; Ulubayram, K. *Polymer* **2006**, *47*, 6931–6940.
(47) Lubke, C.; Lubke, M.; Whitcombe, M. J.; Vulfson, E. N. *Macromolecules* **2000**, *1433*, 5098–5105.

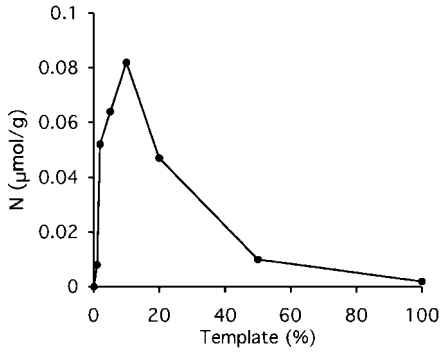

Figure 6. Number of binding sites (*N*) versus varied percent template for measured in experimental MIPs by Spivak and Kim [data was adapted from ref 42].

decreased. (Figure 6) We were interested whether the lattice model simulation could replicate this trend and whether it could assist in establishing its origins.

We repeated Spivak and Kim's experiment utilizing the lattice model simulation. The monomer and cross-linking agent concentrations and the K^* term were held constant ([M] = 7.81%, [CL] = 31.25%, and $K^* = 33.3$). Again, these values were chosen to mirror the experimental conditions. The concentrations of template were varied from 0 to 100%. The percent template was defined by Spivak and Kim as [T]/([CL] + [M]). The different types of binding sites in each *s*MIP were tabulated (Figure 7). The results mirror those trends observed by Spivak. The population of high-affinity binding sites in the *s*MIPs (types 2, 3, 4) initially increases with increasing template concentration. After reaching a maximum, the population then decreases with the increase of the template concentration. (Figure 7b,c)

The simulation also gave insight into the origins of these trends. Spivak hypothesized that the observed trends were due to the statistical preferences, and the simulation analyses appear to confirm this explanation. At low template concentrations, the monomer units out number the template units, which facilitates the formation of higher order complexes with 4:1, 3:1, and 2:1 monomer−template stoichiometries. Due to La Chatelier's principle, increasing the template concentration initially increases the population of these higher order complexes. However, increasing the template concentration beyond a certain point leads to a decrease in the higher order complexes because the template units start to out number the monomer units. Under these conditions, the lower order 1:1 monomer−template complexes become statistically favored. This is evident in the simulation by the dramatic increase in the number of low-affinity (type 1) binding sites beyond template concentrations of 10% (Figure 7a). The preferential formation of 1:1 complexes at higher template concentrations leads to a decrease in the population of high-affinity binding sites due to mass balance. The point at which this transition occurs differs depending upon the binding constant. When the microscopic binding constant K^* was varied, the concentration of template that yielded the highest population of high-affinity binding sites also shifted. Spivak and Kim observed the same trends with different template molecules. Each template had a different binding affinity (and also stoichiometry) for the monomer and thus the optimal template concentration varied accordingly. These studies demonstrate again that there is a competition between the formation of low-affinity and high-affinity binding sites for the monomer units. If the population of one type of binding sites increases then there must be an accompanying decrease in the population of other types of binding sites.

We were interested in whether polymers formed with higher affinity monomers would have similar trends to those formed using the traditional lower affinity monomers. This is of particular interest as functional monomers with increasingly higher association constants have recently been developed and applied to the molecular imprinting process.[48] However, experimental studies on the optimal formulations for these higher affinity polymers have not been reported. Thus, the effect of template concentration on the binding capacities of three *s*MIPs ($K^* = 10$, 100, and 1000) were examined. The simulated polymers utilized the same imprinting conditions as the previous studied *s*MIP ($K^* = 33.3$), and the number of high-affinity binding sites (N_{HBS}) in these *s*MIPs was calculated at various template concentrations (Figure 8). In this study, the high-affinity binding sites were defined as the type 2, 3, and 4 binding sites. Similar trends were observed for all three polymers, mirroring those in the previous study. At low template concentrations (<10%), an increase in template concentration led to the formation of more high-affinity binding sites. This trend reaches a maximum at a template concentration of between 10% and 30% and then drops. However, clear differences were seen in the slope of this maximum for the three polymers. In the low-affinity *s*MIP ($K^* = 10$), the maximum is very low and broad. This suggests that the binding capacity is not that sensitive to variations in the template concentration. However, the high-affinity *s*MIP ($K^* = 1000$) showed a very sharp maximum. This suggests that there is a very narrow range of optimal monomer−template ratios for these high-K^* MIPs. Thus, the optimization of the template concentrations in these high-K^* MIPs should be carried out very carefully as very small variations in the template concentration will lead to large changes in binding capacities of the corresponding MIPs.

4. Simulation of Selectivity Trends in MIPs. The above simulations examined the binding capacities, affinities, and heterogeneous distributions of MIPs. However, the most important binding property of MIPs is their selectivities and in particular enantioselectivities.[8,9] Imprinted polymers prepared using chiral templates have been shown to be highly enantioselective. Furthermore, the enantioselectivity can be rationally tailored by use of a particular enantiomer as the templating agent. We were interested whether the lattice model simulation could be extended to study the selectivity in MIPs.

For the selectivity simulations, a template that has only two binding faces was used (Figure 9). There are various "isomeric" forms of a two-sided template. We chose "isomers" that have one binding face in common and labeled them left and right isomers. This would be analogous to the situation with enantiomeric templates that present the same number and geometric arrangements of binding functional-

(48) Wulff, G.; Knorr, K. *Bioseparation* **2001**, *10*, 257–276.

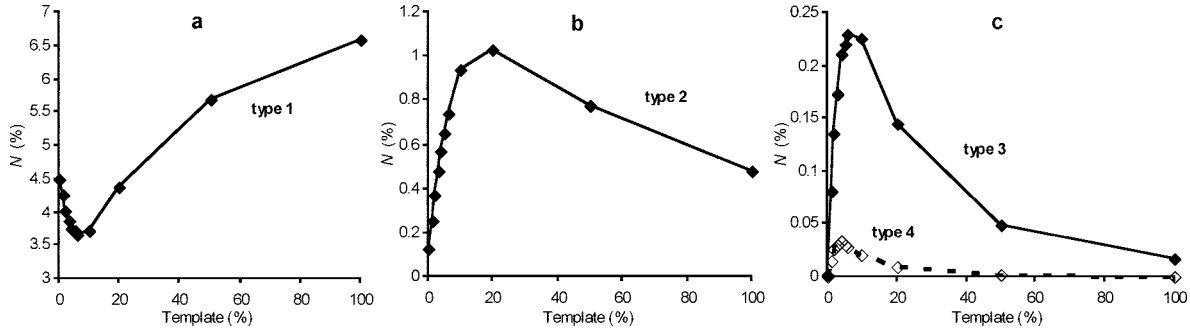

Figure 7. Number of binding sites versus varied percent template in *s*MIPs ($K^* = 33.3$) for type 1 (a), type 2 (b), and type 3, 4 (c) binding sites.

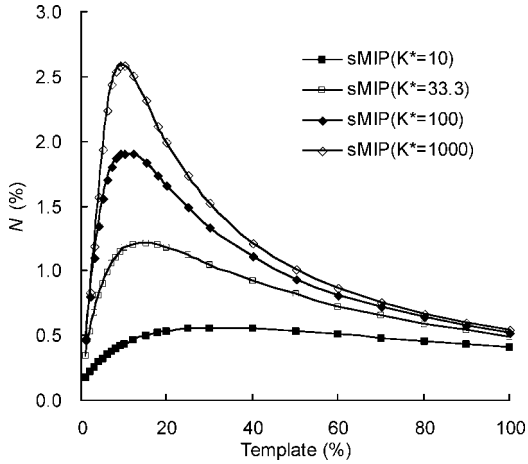

Figure 8. Number of high-affinity binding sites versus varied percent template in *s*MIPs.

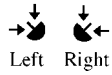

Figure 9. Isomeric template units used in *s*MIP selectivity studies.

ities. The simulation was run as before using one of the isomeric templates. The simulated polymers could then be assessed for the number and types of binding sites that were complementary to each isomeric template unit. In this simulation, there are two types of binding sites because the template has only two binding faces. The low-affinity binding sites have only one functional monomer that can bind to the template. The high-affinity binding sites contain two functional monomers that can bind to the template.

The first selectivity studies examined whether an *s*MIP formed with one isomer would show selectivity for the templated isomer over its antipode. The simulation was run under similar conditions to the previous studies ([T] = 1.95%, [M] = 7.81%, [CL] = 31.25%). The right isomer was selected as the template. An imprinted and nonimprinted polymer were simulated (*s*MIP-right and *s*NIP) by varying the binding constant ($K^* = 50$, $K^* = 1$). Again, these conditions were chosen to parallel the conditions that are commonly used in experimental studies of MIPs. The binding sites were analyzed for their complementarity to each isomer. These results are shown below in Figure 10.

The distribution of binding sites in each polymer is similar to the simulations with the four sided templates. The only difference is that there are only two types of binding sites. The low-affinity binding sites again make up the majority of binding sites. *s*MIP-right has more high-affinity and low-affinity binding sites for the template isomer than *s*NIP (Figure 10a), which is consistent with the observation of an imprinting effect. Next, selectivity studies on *s*MIP-right were carried out. The empty spaces in *s*MIP-right simulation were assessed for their affinity for the matched and unmatched isomers. The selectivity trends mirror those observed in actual MIPs. *s*MIP-right showed selectivity for the templated right-isomer over the left-isomer (Figure 10b). Interestingly, *s*MIP-right has a similar number of low-affinity binding sites for each isomer. However, clear differences in capacity are seen for the high-affinity binding sites. *s*NIP showed no selectivity (not shown) as it contained the same number of binding sites for each isomer.

Further study and comparison to published works required conversion of the simulated affinity distributions into chromatographic selectivity parameters. Spivak's study was one of the few that measured the population of binding sites.[42,49] In contrast, the majority of studies on the imprinting effect have been measured using the chromatographic separation factor (α). The number of low and high-affinity binding sites complementary to each isomer was converted into selectivity factors using eqs 5 and 6. Equation 5 is the bi-Langmuir isotherm that calculates the binding capacity (B) from the number of binding sites (n_i) and binding constant (K_i). The numbers of the low- and high-affinity binding sites were taken directly from the simulation. Here [G] is the free concentration of analyte concentration. A couple of different [G]s were chosen for comparison (Figure 10a). The binding constants (K_1 and K_2) of high- and low-affinity binding sites were estimated to be 2500 and 50. These values were selected based on the assumption that the binding contributions of each monomer to a binding site are additive. Thus, the $K_1 = K^*$ and $K_2 = K^{*2}$. The separation factor (α) is the ratio of binding capacities of a polymer for analyte one (B_1) over analyte two (B_2; eq 6).

$$B = \frac{n_1}{1 + \frac{1}{K_1[G]}} + \frac{n_2}{1 + \frac{1}{K_2[G]}} \tag{5}$$

$$\alpha = \frac{B_1}{B_2} \tag{6}$$

The effect of the monomer/template ratio on the separation factor has been experimentally studied for MIPs imprinted

(49) Huang, X. D.; Zou, H. F.; Chen, X. M.; Luo, Q. Z.; Kong, L. *J. Chromatogr., A* **2003**, *984*, 273–282.

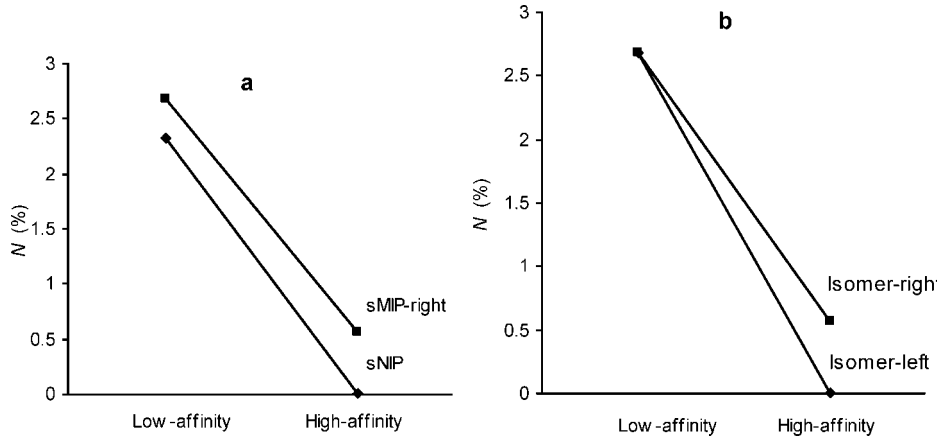

Figure 10. (a) Comparison of the numbers of low-affinity and high-affinity binding sites for the right isomer in *s*NIP and *s*MIP-right; (b) comparison of the numbers of low-affinity and high-affinity binding sites for the left and right isomers in *s*MIP-right.

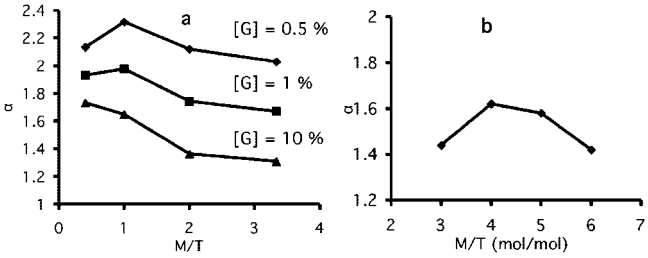

Figure 11. (a) Effect of molar ratios of monomer to template in a *s*MIP on the separation factor (α) at different guest concentrations: [G] = 0.5% (filled diamond), [G] = 1% (filled square), [G] = 10% (filled triangle). (b) Effect of molar ratios of monomer to template reported in the literature for phenylalanine anilide MIPs [data was adapted from ref 50].

with *L*-phenylaniline anilide.[50] In this study, an optimal M/T ratio was observed that yielded the highest separation factor (Figure 11b). We sought to reproduce this study by using the lattice model simulation. The simulation was run under similar conditions to the previous studies ([M] = 7.81%, [CL] = 31.25%). A series of imprinted polymers were simulated with a binding constant of $K^* = 50$ by varying the template concentration. First, the separation factor of the *s*MIP increases with the template concentration (Figure 11a). The α value reaches a maximum and then decreases at high template concentrations. This effect becomes more pronounced at lower [G]s where *s*MIPs show the highest selectivities at low analyte concentrations. More importantly, under these low analyte concentration conditions, the *s*MIPs showed an optimal M/T ratio similar to the experimentally measured trends. The differences in the absolute values of α between the experimental and simulated polymers are due to differences in the binding constants of the two experiments.

This study highlights one of the advantages of a stoichiometric model. The rules of the stochastic model can be easily changed to examine different variables and conditions. The selectivities of MIPs were examined by changing the rules in the stochastic model, and the results favorably replicated the experimentally observed trends.

This stochastic study of the imprinting process does share many characteristics with studies of the imprinting process macroscopic equilibrium equations.[51,52] However, the lattice model simulation has a number of unique features and advantages. First, the binding sites in the lattice model are formed both via the formation of monomer−template complexes and randomly. The random formation of binding sites is consistent with large number of binding sites observed in nonimprinted materials and also their similar highly heterogeneous distributions. Second, the lattice model simulations can be visually monitored, which allows the examination of the origins each binding site and BSH. Finally, the stochastic model also takes into account the physical interaction of the monomer units in the polymerization process. The monomers and cross-linkers can physically occupy and block binding sites. This enables the lattice model to simulate polymeric properties of the MIPs and also the unique high concentration conditions that are used in their formation.

To simplify the simulations, many generalizations and assumptions were made about the nature of the imprinting process that may not accurately represent the imprinting conditions in every imprinted polymer. For example, a key assumption in this model was that higher order complexes with stoichiometries greater than 1:1 (monomer:template) are commonly formed in MIPs. This is probably true in many MIPs, however, studies have shown that chiral templates that can interact with only one monomer can still yield a strong imprinting effect as demonstrated by the enantioselectivity of the resulting MIPs.[53] In these systems, shape selectivity appears to play an important role in the recognition process.[54,55] Although our stochastic model does not explicitly take into account the possibility of shape selectivity arising from steric interactions, the role of the second, third, and fourth monomer can be thought of as parts of the polymer matrix that provide some degree of shape selectivity as they can modulate the affinity of a binding site for the template molecule. The ability of the second and third

(50) Lin, J. M.; Nakagama, T.; Uchiyama, K.; Hobo, T. *Chromatographia* **1996**, *43*, 585–591.
(51) Whitcombe, M. J.; Martin, L.; Vulfson, E. N. *Chromatographia* **1998**, *47*, 457–464.
(52) Svenson, J.; Andersson, H. S.; Piletsky, S. A.; Nicholls, I. A. *J. Mol. Recognit.* **1998**, *11*, 83–86.
(53) Spivak, D. A.; Simon, R.; Campbell, J. *Anal. Chim. Acta* **2004**, *504*, 23–30.
(54) Spivak, D. A.; Campbell, J. *Analyst* **2001**, *126*, 793–797.
(55) Simon, R.; Collins, M. E.; Spivak, D. A. *Anal. Chim. Acta* **2007**, *591*, 7–16.

monomers to provide shape selectivity can be seen by the ability of the simulated polymers to distinguish the isomeric templates in the simulations of MIP selectivity.

Conclusions

The initial goal of this study was to test whether a link could be established between BSH in MIPs and the heterogeneity in the prepolymerization solution. This was tested by developing a molecular imprinting simulation based solely on the monomer−template equilibrium in the prepolymerization solution. The simulated affinity distributions closely paralleled experimentally measured affinity distributions in MIPs. This suggests that the monomer−template equilibrium is a major source of BSH as hypothesized.

The lattice model simulation was also able to accurately replicate other trends that have been experimentally measured for MIPs including the imprinting effects, binding site distributions, and selectivities. More interestingly, the simulation gave insight into the origins of the imprinting effect and suggested new routes for their improvement. For example, a key mechanism in the imprinting process is the partitioning of the binding sites between low- and high-affinity binding sites. Thus, the enhancement in the number of one type will lead to a direct decrease in the other type. Another observation that arose from this study was a new method for enhancing the imprinting effect by reducing the number of randomly formed sites. The use of cross-linkers or monomers that bind to monomer units that are not bound to template units can greatly reduce the population of low-affinity binding sites. The weak interactions between the cross-linker and the monomer and the self-association of monomers may help the reduction of low-affinity background binding sites, and we are currently developing a model that can simulate these intramolecular and intermolecular interactions. The stochastic model simulation also suggested that the optimization of high-affinity MIPs needs to be done more carefully because these polymers are very sensitive to the imprinting variables in a very narrow range.

Acknowledgment. The authors of this paper would like to thank the National Institutes of Health (GM062593) and the National Science Foundation (0616442) for financial support.

Supporting Information Available: Details of the studies comparing the equilibrium calculations of the stochastic simulation with calculations based on the macroscopic equilibrium equations and a flowchart of the simulation program (PDF). This material is available free of charge via the Internet at http://pubs.acs.org.

CM8002645